SERBIAN JOURNAL OF ELECTRICAL ENGINEERING
Vol. 10, No. 2, June 2013, 261-274

UDK: 621.354.322 **DOI: 10.2298/SJEE120707003M**

Comparative Study of a Small Size Wind Generation System Efficiency for Battery Charging

Messaoud Mayouf[1], Rachid Abdessemed[1]

Abstract: This paper presents an energetic comparison between two control strategies of a small size wind generation system for battery charging. The output voltage of the direct drive PMSG is connected to the battery through a switch mode rectifier. A DC-DC boost converter is used to regulate the battery bank current in order to achieve maximum power from the wind. A maximum power-tracking algorithm calculates the current command that corresponds to maximum power output of the turbine. The DC-DC converter uses this current to calculate the duty cycle witch is necessary to control the pulse width modulated (PWM) active switching device (IGPT). The system overview and modeling are presented including characteristics of wind turbine, generator, batteries, power converter, control system, and supervisory system. A simulation of the system is performed using MATLAB/SIMULINK.

Keywords: Battery charging, Permanent magnet synchronous generator (PMSG), Maximum power point tracking (MPPT), PWM DC-DC boost converter

1 Introduction

Variable speed wind turbines have many advantages over fixed speed generation such as increased energy capture, operation at maximum power point, improved efficiency and power quality [1]. However, the presence of gearbox matching the wind turbine to the generator still causes problems. The gearbox suffers from faults and requires regular maintenance. The reliability of the variable speed wind turbine can be improved significantly by using a direct drive permanent magnet synchronous generator. PMSG has received much attention in wind energy application because of its property of self-excitation, which allows operations at high power factor and high efficiency [2].

A wind energy conversion system with PMSG can be used basically in three distinct applications: standalone systems, hybrid systems, and grid connected systems [3]. For a standalone system, the output voltage of the load

[1]Department of Electrical Engineering, Faculty of Engineer's Sciences, Batna University, Algeria;
E-mails: mayouf71@yafoo.fr; rachid.abdessemed@gmail.com

side converter has to be controlled in terms of amplitude and frequency. Previous publications related to PMSG based variable speed wind turbine are mostly concentrated on grid connected system, and MPPT control strategies are often based on the estimation of PMSG electromagnetic torque [1 – 2]. For electric generation in isolated systems, many countries are affluent in renewable energy resources; however they are located in remote areas where power grid is not available. To resolve this problem, small wind turbines for battery charging are very useful. However, cost effectiveness is very important for such applications and topologies used for higher power generation are not viable [3 – 4].

The direct connection of a three-phase diode controlled rectifier to the batteries is a common practice adopted by some manufactories; Although there is simplicity and robustness, several problems associated with this solution result, such as the reduction of batteries useful life and increase of power losses [5], also, the wind turbine does not operate in its maximum electrical power in all operating conditions. Therefore, it is necessary to provide variable wind generation configuration; which allows the use of wind turbine for its maximum power coefficient in large wind speed range, and optimizes the use of the available wind energy. This is possible by inserting a DC-DC converter between the rectifier and the battery, to adapt the generator voltage to the battery bank voltage [5 – 6]. In reference [5], two regulation loops are used in the control system, an external controller regulates the output voltage to avoid overvoltage, and internal controller regulates average inductor current to achieve the maximum power point. However, we will focus in this paper on the energetic behavior comparison of the wind conversion topology studied, using proposed MPPT algorithms for power maximizing, with and without speed sensor. Thus, we will reduce the control system to one controller. The purpose of this comparison is to deduce by the end of this paper, the appropriate choice that we offer efficiency, simplicity, and with lower cost.

2 System Configuration

The proposed system is shown in Fig. 1. It is composed of a vertical axis wind turbine directly connected to a permanent magnet synchronous generator. The generator is cascaded with a battery charger composed by a three-phase rectifier and a DC-DC boost converter. In order to know the global behavior of the production system, we suppose that the batteries are composed of an ideal electric supply source E_{bat} in series with a resistance R_{bat}. The battery charger operates to obtain maximum power transferred to the batteries. The converter duty cycle is changed in accordance with control system which receives a reference signal from the supervisory system.

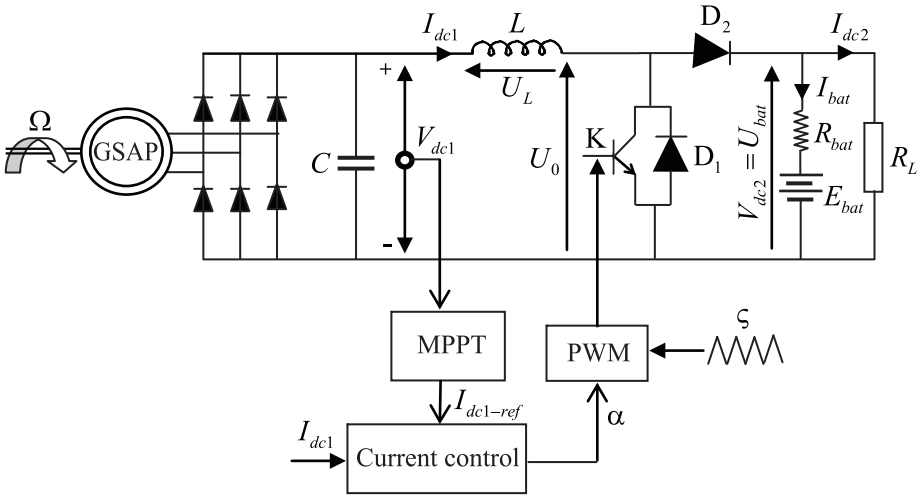

Fig. 1 – *General scheme of the proposed system.*

3 System Modeling

In order to develop the simulation model that achieves the objectives of this work, a quite detailed methodology has been solicited. The simulation scheme has been implanted after the modeling of all parts constituting the wind power system, and the development of the proposed algorithms through analytical equations. The models used for turbine, generator, batteries, and rated values adopted in the designed system are based on the steady state characteristics of the vertical axis wind turbine, thy are presented and discussed as follows:

3.1. Wind turbine model

The output mechanical power available from a wind turbine can be expressed as follows:

$$p_m = \frac{1}{2}\rho S C_p(\lambda) V_v^3, \tag{1}$$

with

$$\lambda = \frac{R\Omega}{V_v}, \tag{2}$$

where ρ is the air density (typically 1.225kg/m^3 at sea level with standard conditions, i.e. temperature of 15°C and atmospheric pressure of 101.325kpa), S is the area swept by the rotor blades (in m^2), V_V is the wind speed (in m/s), and C_p is the so-called "power coefficient" of the wind turbine (dimensionless), with R being the radius of the turbine blades (in m), and ω being the angular speed of

the turbine rotor (in rad/s). As can be derived from (1), the power coefficient C_p is a nonlinear function of the tip-speed ratio TSR or λ (dimensionless). Therefore, if the air density, swept area, and wind speed are constant, the output power of the turbine will be a function of the turbine power coefficient. A generic equation is used to model the power coefficient $C_p(\lambda)$, based on the modeling of vertical axis turbine characteristics used in [6]:

$$C_p = -0.2121\lambda^3 + 0.0856\lambda^2 + 0.2539\lambda \,. \tag{3}$$

The characteristic function $C_p(\lambda)$, is illustrated in Fig. 2.

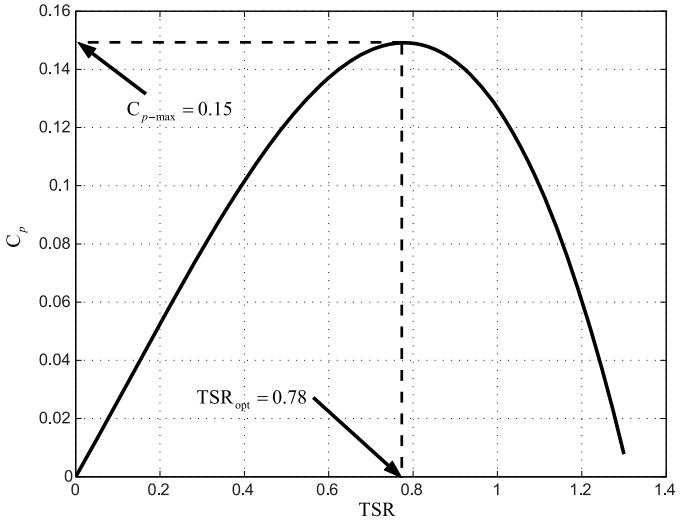

Fig 2 - *Power coefficient versus tip-speed ratio.*

As can be seen from Fig. 2, at TSR_{opt}, C_p has its maximum value which results in the optimum efficiency. For each wind speed, there exists therefore, a specific point in the wind generator power characteristic; this point is known as the maximum power point (MPPT), where the output power is maximized. Thus, the control of the wind energy conversion system enables variable-speed operation of the turbine, such that the maximum power is extracted continuously from the wind. The target optimum power from a wind turbine can be written as:

$$P_{m-opt} = \frac{1}{2}\rho S C_{p-opt}\left(\frac{R\Omega_{opt}}{\lambda_{opt}}\right)^3 = K_{opt}\Omega_{opt}^3 \,, \tag{4}$$

where

$$K_{opt} = \frac{1}{2}\rho S C_{p-opt}\left(\frac{R}{\lambda_{opt}}\right)^3, \tag{5}$$

and

$$\Omega_{opt} = \frac{\lambda_{opt}}{R}V\ . \tag{6}$$

3.2. Generator model

Permanent magnet synchronous generator with sinusoidal distribution of conductors can be represented in the rotor reference frame as:

$$\begin{aligned} V_d &= -R_s I_d - L_d \frac{d}{dt} I_d + \omega L_q I_q, \\ V_q &= -R_s I_q - L_q \frac{d}{dt} I_q - \omega L_d I_d + \omega \psi_f, \end{aligned} \tag{7}$$

where:

L_d : Stator inductance in direct axis **[**H].

L_q : Stator inductance in quadrature axis [H].

R_S : Stator phase winding resistance [Ω].

ψ_f : Amplitude of the flux linkages [vs/rad].

The electromagnetic torque is expressed by:

$$C_{em} = \frac{3}{2}P[(L_q - L_d)i_d i_q + i_q \psi_f] \tag{8}$$

and P is the number of pole pairs of PMSG.

The machine dynamics is given by the following mechanical equation:

$$C_m - C_{em} - f\Omega = J\frac{\mathrm{d}\Omega}{\mathrm{d}t}, \tag{9}$$

where:

C_m : motor torque developed by the turbine shaft [Nm],

C_{em} : electromagnetic torque developed by the generator [Nm],

$f\Omega$: friction torque,

J: moment of inertia reported to the generator shaft [kgm^2],

f: friction coefficient,

Ω: mechanical angular velocity of the turbine [rad/s].

The relation between the rotor angular velocity of the generator ω and the mechanical angular velocity of the wind turbine rotor Ω is expressed as:

$$\omega = \frac{P}{2}\Omega . \tag{10}$$

The diode rectifier is the most commonly used topology in power electronic applications. For a three phase system, it is consisting of six diodes. The diode rectifier may be used only in one quadrant; it is simple, and it is not possible to control it. The dc voltage and current output depend on the generator voltage and current as following:

$$v_{dc1} = \frac{3}{\pi} E_{ab}^{\max} = \frac{3\sqrt{6}}{\pi} \psi_{f-eff} P\Omega , \tag{11}$$

$$I_{dc} = \frac{\pi}{\sqrt{6}} I_g , \tag{12}$$

where V_{dc1} and I_{dc1} are medium output voltage and current of rectifier, and E_a and I_g are output voltage and current of generator (phase *a*).

3.3. Battery model

The battery bank model adopted is formed by an ideal voltage supply E_{bat} in series with resistance R_{bat}. The inclusion of such resistance is very important because it causes the battery bank voltage ripple. The resistance value is calculated according to the battery nominal voltage. For example, a lead battery resistance is given by the following expression [6]:

$$R_{bat} = N \cdot 0.036\,\Omega , \tag{13}$$

where *N* is the number of elementary cells number with nominal voltage of 12V.

3.4. Boost Converter Model

The standard unidirectional topology of the DC-DC boost converter of the Fig. 1, consist of a switching-mode power device containing basically two semiconductor switches (a rectifier diode D_2 and a power transistor K with its corresponding anti-parallel diode D_1) and an inductor *L*. The output DC voltage is produced at a level higher than its input DC voltage. This converter acts as an interface between the full-wave rectifier bridge and the battery bank, by employing pulse-width modulation (PWM) control techniques. Operation of the DC-DC converter in the continuous (current) conduction mode (CCM), i.e. the current flowing continuously in the inductor during the entire switching cycle, facilitates the development of the state-space model because only two switch states are possible during a switching cycle, namely, (i) the power switch K is on and the diode D_2 is off; or (ii) K is off and D_2 is on. Electric equations that

describe the dynamics of the DC-DC boost converter over a commutation period are given by:

$$V_{dc2} = \frac{1}{1-\alpha} V_{dc1}, \tag{14}$$

$$I_{dc2} = (1-\alpha) I_{dc1}, \tag{15}$$

$$v_{dc1} = U_0 + U_L, \tag{16}$$

where I_{bat} is the converter output current (battery current charging), U_{bat} is the output voltage, v_{dc1} is the boost converter input voltage, U_L and U_{d0} are respectively, inductor (L) and power switch (K) voltages.

We define R_g, and R_{dc1} as a variable resistances of whole circuit located respectively, upstream and downstream of the rectifier, they vary depending on the duty cycle, and load resistance R.

Currents I_{dc1} and I_{dc2} are given by:

$$I_{dc1} = \frac{V_{dc1}}{R_{dc1}}, \tag{17}$$

$$I_{dc2} = \frac{V_{dc2}}{R_L}. \tag{18}$$

Based on the conservation energy principle, we can write:

$$R_g I_g^2 = R_{dc1} I_{dc1}^2 = R_L I_{dc2}^2, \tag{19}$$

$$R_g I_g^2 = R_{dc1} \frac{\pi}{\sqrt{6}} I_g^2 = R_L (1-\alpha)^2 \frac{\pi}{\sqrt{6}} I_g^2. \tag{20}$$

We deduce then, the expression of the resistance R_g:

$$R_g = \frac{\pi^2}{18} (1-\alpha)^2 R_L. \tag{21}$$

In order to get the maximum power extracted from the generator, we will express the power supplied by the generator as a function of duty cycle. The electric power supplied by the generator is given by:

$$P_g = 3R_g \frac{E_g^{\ 2}}{(R_s + R_g)^2 + X_s^{\ 2}}. \tag{22}$$

By replacing R_g and R_S by their expressions, we can express the power P_g by:

$$P_g = \frac{\pi}{6} (1-\alpha)^2 R_L \frac{(k\psi_{eff}\Omega)^2}{\left[\frac{\pi}{18}(1-\alpha)^2 R_L + R_S\right]^2 + X_S^{\ 2}}. \tag{23}$$

The search of the maximum power $P_{g\text{-max}}$ is equivalent to the search of duty cycle canceling its derivative, which gives:

$$1-\alpha_{opt}=\frac{3}{\pi}\sqrt{\frac{2\sqrt{R_S{}^2+X_S{}^2}}{R_L}}\,. \tag{24}$$

Maximum power $P_{g\text{-max}}$ is therefore given by:

$$P_{g-\max}=\frac{3(k\psi_{eff}\Omega)^2\sqrt{R_S{}^2+X_S{}^2}}{(\sqrt{R_S{}^2+X_S{}^2}+R_S)^2+X_S{}^2}\,. \tag{25}$$

4 Control of DC-DC Boost Converter with Maximum Power Extraction

The DC-DC boost converter input current can be controlled by controlling the duty cycle of the switch (K), at any wind speed to extract maximum power from the wind turbine. Fig. 5 shows the control block diagram of DC-DC boost converter.

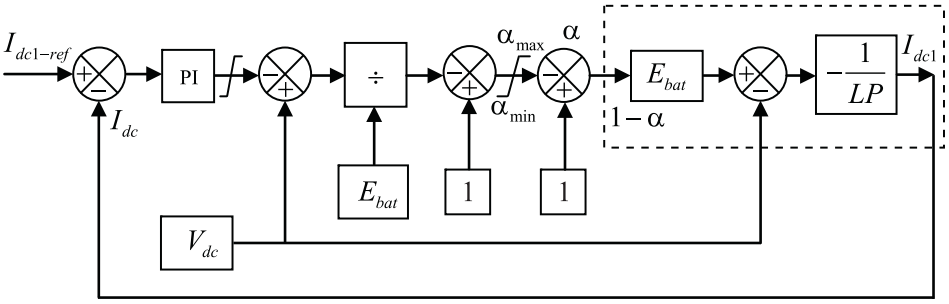

Fig. 5 – *Control block diagram off* DC-DC *boost converter.*

It is possible to simplify the control block diagram in Fig. 5 by eliminating clearing and disturbance terms. The reduced scheme is shown in Fig. 6.

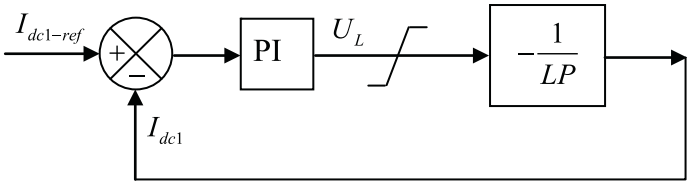

Fig. 6 – *Simplified diagram of control loops.*

Since the boost converter input current I_{dc1} depends on the power P_{dc1}, we can consider this power as reference state variable according to following relation:

$$I_{dc1}^{ref} = \frac{P_{dc}^{ref}}{V_{dc1}}. \tag{26}$$

4.1 Control strategy with speed sensor

The regulating current I_{dc1} depends on the power P_{dc1} which is selected as variable reference, and the measurable voltage V_{dc1}. From (4) and (11) giving optimal wind power P_{opt} and voltage V_{dc1}, according to the rotor speed, it is possible to express the reference current $I_{dc1\text{-}ref}$ using the following expression:

$$I_{dc1-ref}(\Omega) = \frac{P_{opt}}{V_{dc1}} = \frac{\frac{C_p^{\max}}{\lambda_{opt}}\rho R^4 H \Omega^3}{\frac{3\sqrt{6}}{\pi}\psi_{eff} P\Omega}, \tag{27}$$

$$I_{dc1-ref}(\Omega) = \frac{\pi C_p^{\max}\rho R^4 H}{3\sqrt{6}\lambda_{opt}\psi_{eff} P} = \delta\Omega^2, \tag{28}$$

where δ is a constant defined by:

$$\delta = \frac{\pi C_p^{\max}\rho R^4 H}{3\sqrt{6}\lambda_{opt}\psi_{eff} P}. \tag{29}$$

The control algorithm includes therefore the following steps:
– measure rotor speed,
– determine input reference current of DC-DC boost converter.

4.2 Sensorless Control strategy

The senseless control strategy proposed in this work is based on the indirect piloting of the battery current charging, without knowing either the wind speed or the wind turbine speed. This can simplify the wind power conversion system and minimize its cost, without reducing the energetic efficiency. Knowing that electromotive force of PMSG is expressed in terms of rotor speed; the mechanical speed sensor can be suppressed and replaced by a simple voltage measure, which can be assimilated to the rotation speed according to following equation:

$$v_{dc1}(\Omega) = \frac{3}{\pi}E_{ab}^{\max} = \frac{3\sqrt{6}}{\pi}\psi_{f-eff} P\Omega = \mu\Omega, \tag{30}$$

where μ is a constant given by:

$$\mu = \frac{3\sqrt{6}}{\pi}\psi_{f-eff}P\,. \tag{31}$$

Using (28) and (30), it is possible to express the target optimum boost converter input current $I_{dc1\text{-}ref}$ according to the voltage V_{dc1} by:

$$I_{dc1-ref}(\Omega) = \delta\Omega^2 = \delta\left(\frac{V_{dc1}}{\mu}\right)^2 = \beta V_{dc1}^2\,, \tag{32}$$

where μ is a constant given by:

$$\beta = \frac{\delta}{\mu^2} = \pi C_p^{\max}\rho R^4 H\left(\frac{\pi}{3\sqrt{6}\lambda_{opt}\psi_{eff}\,p}\right)^3. \tag{33}$$

The control algorithm includes therefore the following steps:
– measure output diode rectifier voltage,
– determine the boost converter input reference current.

For an optimal working regime, the output rectifier voltage value can be determined according to the wind speed by the following expression:

$$V_{dc1} = \frac{3\sqrt{3}}{\pi}p\psi_{f-\max}\frac{\lambda_{opt}}{R}V_v\,. \tag{34}$$

Neglecting losses, the output rectifier voltage can be written according to the battery voltage U_{bat} and duty cycle α by:

$$V_{dc1} = (1-\alpha)U_{bat}\,. \tag{35}$$

According to the wind system application conditions, the simple DC-DC boost converter imposes some limitations. The converter input voltage possesses minimal and maximal stops, determined by the battery voltage U_{bat} and duty cycle stops $\alpha_{\min}$ and $\alpha_{\max}$.

The minimum input voltage of DC-DC converter is defined by:

$$V_{dc1}^{\min} = (1-\alpha_{\max})U_{bat} = \frac{3\sqrt{3}}{\pi}p\psi_{\max}\frac{\lambda_{opt}}{R}V_v^{\min}\,. \tag{36}$$

Therefore, the minimum wind speed can be calculated according to the battery voltage:

$$V_v^{\min} = \frac{(1-\alpha_{\max})U_{bat}\pi R}{3\sqrt{6}\,p\psi_{eff}\lambda_{opt}}\,. \tag{37}$$

Admitting that maximum value duty cycle is equal to 0.99; it is possible to find the minimum wind speed ensuring the good functioning of the wind power conversion system for different battery voltages. For a battery voltage equal

300 V, the minimum wind speed is: $V_v^{\min} \approx 0.32$ m/s . For the duty cycle lower limit that is supposed equal to 0.1, there is no problem posed, because the wind values gotten are very big.

5 Results and Discussions

The model of the variable speed wind turbine system with PMSG is shown in Fig. 7; it is built using Matlab/Simpower dynamic system simulation software.

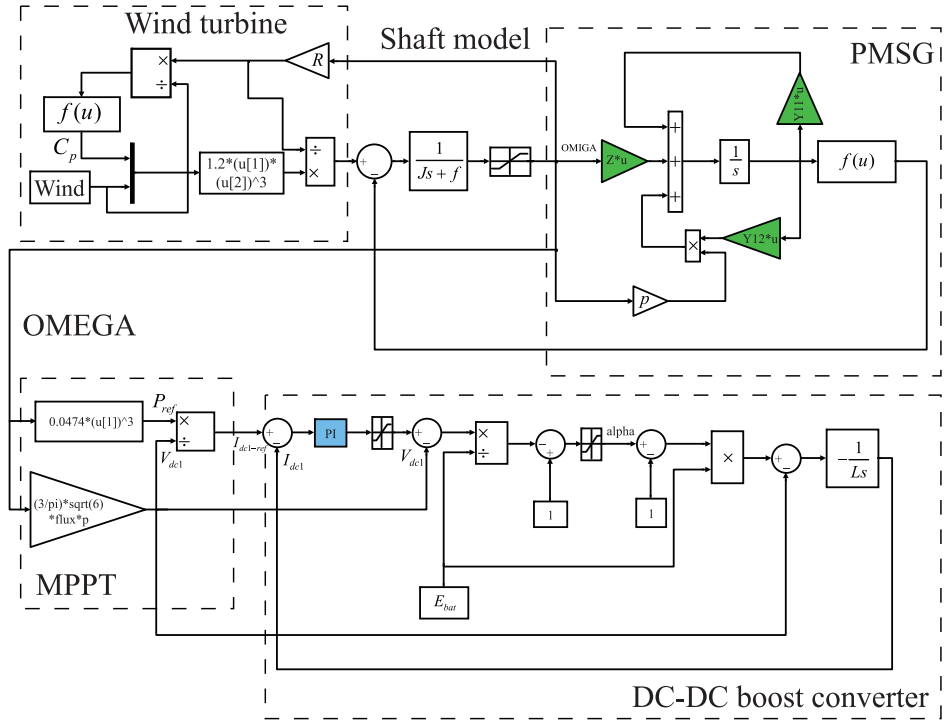

Fig. 7 – *Schematic of the simulated circuit.*

The system simulation is obtained considering the expressions presented in the previous sessions, power converter and control algorithms are also implemented and included in the model. The simulations have the objective to prove and to validate the existence of an optimum point of operation and to predict the behavior system for each wind speed. The wind profile used during this study is shown in Fig. 8. As shown in Fig. 9, powers supplied with MPPT control strategies follow the wind speed profile, and they are close to the optimal power for each variation of wind speed. At low speed, the turbine does not produce energy, because the induced voltage in the PMSG will not be high

enough to overcome the reverse bias in the diode bridge. As the wind speed decreased or increased, the speed sensor controller tracks maximum power slightly better than senseless controller.

The integrated value of the maximum power at the end of the simulation is the maximum energy available from the wind with this system. Simulation results show that the overall energy captured is optimized by the control strategy throughout the range of wind speed as can be seen in Fig. 10.

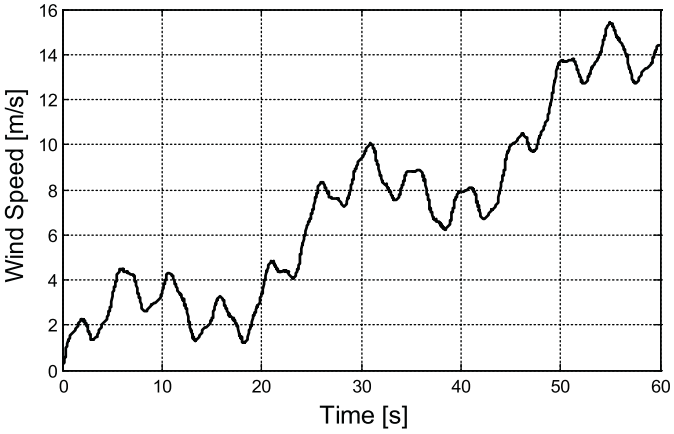

Fig. 8 – *Wind profile used for system simulation.*

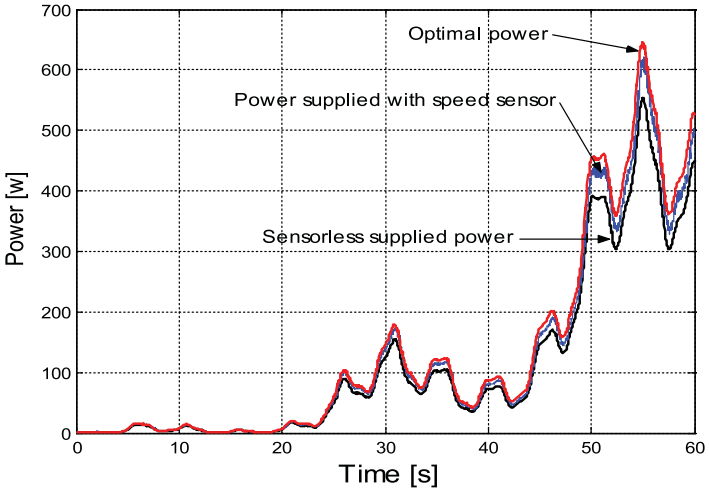

Fig. 9 – *Powers tracking performance of the system.*

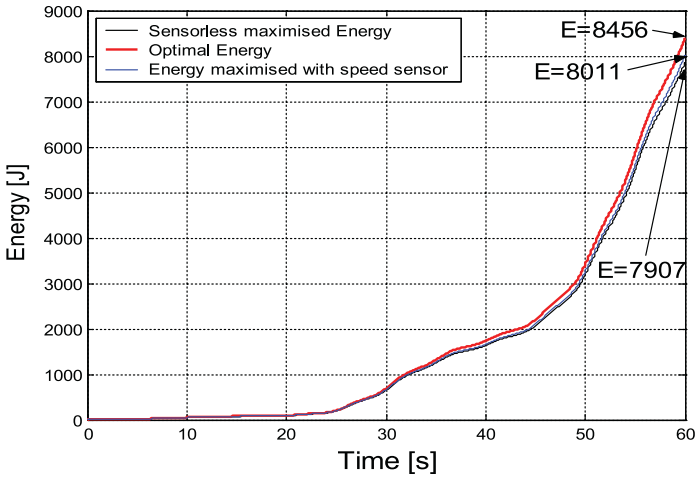

Fig. 10 – *Maximum energy available from the system.*

6 Conclusion

Simple control strategies applied in small size wind generator system for charging batteries have been proposed. A complete modeling and simulation of turbine, generator, converter, and battery was developed. The MPPT system was designed and studied via simulated results. The main target of the proposed system is the exploitation of the available wind energy at low speeds in an optimum operating point without compromising the efficiency at higher wind speeds. Although, the energetic behavior is slightly better in the control strategy with speed sensor; the sensorless control algorithm of DC-DC boost converter is designed without measuring wind and generator speed, which is of great importance for small size and low cost wind turbine. These advantages favor the use of this configuration and control strategy in isolated sites.

Future perspectives for additional studies include development of an MPPT algorithm, tests with prototype using big size wind generation systems.

7 Appendix

Parameters of wind power system:

Wind turbine	
Rated power P [W]	600
Density of air ρ [kg/m^3]	1.225
Area swept by blades S [m^2]	2
Optimum coefficient K_{opt} [Nm/(rad/s)^2]	0.0474

PMSG	
Number of stator poles	34
Rated current [A]	4.8
Rated voltage [V]	90
Armature resistance R_S [Ω]	1.137
Magnet flux linkage [Wb]	0.15
Stator inductance L_S [mH]	2.7
Rated power P [W]	600
Moment of Inertia J [kgm^2]	0.1

DC-DC *converter*	
Filtering voltage capacity C [mF]	3.3
Smoothing inductance L [mH]	2.5
Cutting frequency F_{cut} [kHz]	5
Diode threshold voltage V_D [V]	0.65
Transistor threshold voltage: V_T [V]	0
Diode conduction resistance: R_D [Ω]	$20.7 \cdot 10^{-3}$
Transistor conduction resistance: R_T [Ω]	$85 \cdot 10^{-3}$

8 References

[1] S. Vijayalakshmi, S. Saikumar, S. Saravanan, R.V. Sandip, V. Sridhar: Modelling and Control of a Wind Turbine using Permanent Magnet Synchronous Generator, International Journal of Engineering Science and Technology, Vol. 3 No. 3, March 2011, pp. 2377 – 2384.

[2] M. Yin, G. Li, M. Zhou, C. Zhao: Modeling of the Wind Turbine with a Permanent Magnet Synchronous Generator for Integration, IEEE Power Engineering Society General Meeting, Tampa, FL, USA, 24 – 28 June 2007.

[3] A.M. De Broe, S. Drouilhet, V. Gevorgian: A Peak Power Tracker for Small Wind Turbines in Battery Charging Applications, IEEE Transaction on Energy Conversion, Vol. 14, No. 4, Dec. 1999, pp. 1630 – 1635.

[4] Y. Chen, P. Pillay, A. Khan: PM Wind Generator Topologies, IEEE Transaction on Industry Application, Vol. 41, No. 6, Nov/Dec. 2005, pp. 1619 – 1626.

[5] H.M.O. Filho, D.S. Oliveira, R.P.T. Bascope, C.E.A. Silva, G.J. Almeida: On the Study of Wind Energy Conversion System Applied to Battery Charging using Multiblade Turbine, Brazilian Power Electronics Conference, Bonito, Brazil, 27 Sept. – 01 Oct. 2009, pp. 964 – 971.

[6] A. Mirecki, X. Roboam, F. Richardeau: Comparative Study of Maximum Power Strategy in Wind Turbines, IEEE International Symposium on Industrial Electronics, Ajaccio, France, 04 – 07 May 2004, Vol. 2, pp. 993 – 998.

[7] N.T. Hai, S.H. Jang, H.G. Park, D.C. Lee: Sensorless Control of PM Synchronous Generators for Micro Wind Turbines, 2nd IEEE International Conference on Power and Energy, Johor Bahru, Malaysia, 01 – 03 Dec 2008, pp. 936 – 941.